Analytical Methods

Accepted Manuscript

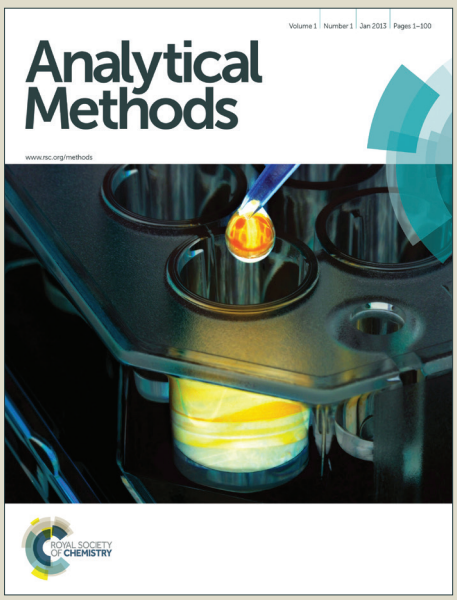

ROYAL SOCIETY OF CHEMISTRY

www.rsc.org/methods

Journal Name

RSCPublishing

COMMUNICATION

Cite this: DOI: 10.1039/x0xx00000x
Received 00th January 2012,
Accepted 00th January 2012
DOI: 10.1039/x0xx00000x
www.rsc.org/

A digital image-based method employing a spot-test for quantification of ethanol in drinks

Luzia Pires dos Santos Benedetti,[a] Vagner Bezerra dos Santos,[a]* Tiago Almeida Silva,[a] Edemar Benedetti Filho,[b] Valdomiro Lacerda Martins[c] and Orlando Fatibello-Filho[a]

A low-cost analytical method for quantification of ethanol in drinks based on the combination of a colorimetric spot-test and a digital image-based (DIB) method is proposed. The digital images from spot-test reactions were captured using a digital camera in a portable plastic chamber designed with internal lighting control. The images were decomposed by a RGB approach using freely available software. The R channel showed the best linearity, with two linear ethanol concentration ranges: from 1.0% to 20.0% v/v (r = 0.999) and from 25.0% to 50.0% v/v (r = 0.980), with limits of detection and quantification of 0.25% and 0.85% v/v, respectively, for the first analytical curve. The developed method was applied to quantification of ethanol in alcoholic drink samples with results in close agreement with those obtained using a spectrophotometric method at a confidence level of 95%, and with low waste generation (835 µL / spot-test). Thus, we believe that the DIB method can be useful regarding to environmental and social impacts, once the method has a low waste generation and uses an easily available instrumentation with potential for *in situ* determination during the alcoholic beverages production and its quality control.

Introduction

Ethanol or ethylic alcohol is a colorless liquid that is miscible in water, and is produced by fermentation or distillation of different biomass feedstocks, such as manioc, corn, sorghum, and sugarcane.[1,2] Ethanol has various applications, *e.g.*, as an industrial solvent in pharmaceuticals, paints, cosmetics, etc., household and hospital disinfectants, and mainly as automotive fuel.[3,4] Moreover, ethanol is present in all alcoholic drinks, being a depressant substance of the central nervous system, capable of causing undesirable changes in the behavior of those who consume it such as euphoria (early stage), lack of coordination, headaches, or even coma (overconsumption).[5,6] The use of ethanol in drinks is legal and widely acceptable, and thus, there is growing concern regarding the control of the purity and levels of ethanol in alcoholic drinks.[7] However, the instrumental cost, as well as the difficulties to handling of samples, has hampered the detection of ethanol in a precise and accurate manner for the quality control of alcoholic drinks.[7]

There are several methods for the determination of ethanol concentration in drinks, which are mainly divided into physical, chemical, and enzymatic methods.[8] In routine analysis, as in the drink industries, ethanol is usually separated from the matrix by a distillation process, and only then it is analyzed using physical or chemical methods.[9] The official method designated by the Association of Official Analytical Chemists (AOAC) for the determination of ethanol in alcoholic drinks is the pycnometry.[10] Despite advantages such as accuracy and that no calibration is required, this method is considered laborious, requiring a calibrated precision balance and a well-controlled laboratory temperature. The AOAC also recommends that measurements of ethanol concentrations in drinks are made by other known physical methods (*e.g.*, refractometry).[10,11] Ethanol oxidation with dichromate in an acid medium is a colorimetric method that is also recommended by the AOAC as an official method.[12]

Other methods such as the spectrophotometry[13-15] and some enzymatic methods have also been employed with success for the determination of ethanol in drinks.[16-18]

A very interesting and inexpensive strategy has been developed and applied in analytical chemistry in recent years: digital image analysis (DIA) or digital image-based (DIB) methods for collecting instantaneous quantitative information about the analyte of interest.[19-27] In this strategy, common digital image-capturing devices such as cameras, webcams, scanners, and cell phones with a built-in camera are used to register images from a colorimetric reaction, *e.g.*, spot-test, in which the intensity of the developed color is directly proportional to the analyte concentration.[28-30] Thus, the analytical signal in this case is related to measurements of light reflected by the surface sample, *i.e.*, reflectance measures, in contrast with typical spectrophotometric or photometric methods that are based on transmittance or absorbance measures.

Most DIB methods employ the RGB color pattern, so called because it makes use of the primary colors (red (R), green (G) and blue (B)), and the fundamental concept that more than 16 million colors can be employed based on various combinations of these[31-33] primary colors. The use of the RGB pattern as an

analytical response is based on the fact that the RGB values change proportionally with color in a colorimetric reaction. Thus, as the color generated during a colorimetric reaction is often associated with the variation in the concentration of a substance of interest, the RGB values can be directly used to perform a quantitative analysis.[32-35] However, capturing the image is not a trivial procedure. In fact, the variability of the light in the environment during this procedure can be the main cause of poor reproducibility in some DIB applications. Indeed, excess light, shadows, *e.g.*, sunny or cloudy weather during the capture of the image could significantly changes the RGB values, and consequently, the concentration of the substance to be analyzed.[26] Thus, a careful procedure should be carried out to overcome this drawback.

In this work, a simple, portable and low-cost chamber with a homogeneous light control based on LED (light-emitting diode) with a coupled digital camera or cell phone with an embedded camera was developed and applied to quantification of ethanol in alcoholic drinks. For this, digital images acquired from a spot-test based on the colorimetric reaction between ethanol and potassium dichromate in an acid medium were treated using an RGB approach. The methodology can be easily performed for analysis of drinks *in situ*, *e.g.*, industry and smallholdings, due to the fast analysis, ease of handling and the low-cost of the apparatus used.

Experimental

Apparatus and instrumentation

The spot-test reactions were conducted in a porcelain plaque containing 12 reaction vessels. Eppendorf (Germany) automatic micropipettes were used for the transfer of exact volumes of reagents and/or samples to the porcelain plaque. The digital images of the colorimetric reactions were obtained using different devices: Sony 12.0 megapixel (MP) digital camera, model Cyber-shot (camera 1); Sony 6.0 MP, model DSC-W50 (camera 2); Fujifilm 5.1 MP, model FinePixA500S (camera 3); Samsung 2.0 MP, model GT-C6112 (camera 4, from a cell phone); and Aony 0.3 MP, model Q9 (camera 5, from a cell phone). For the digital image capture, a closed system ("black chamber", 21 × 15 × 7 cm) was used that was built for accommodation of the porcelain plaque and the digital camera, where the internal light is homogeneously distributed and, thus, ensures the reproducibility of measurements, Fig. 1.

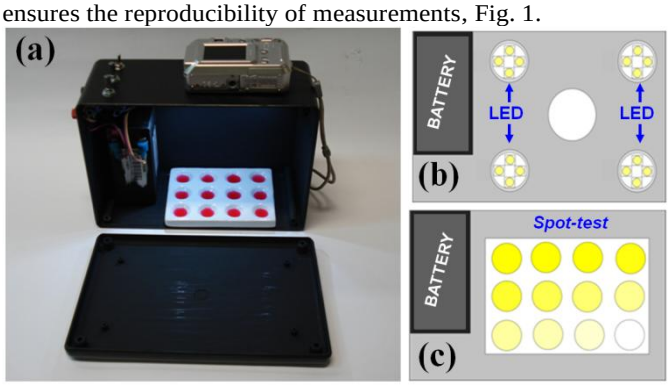

Fig. 1. (a) System built for the image capture. Illustrative representation of the chamber interior used to obtain the images; (b) quantity and arrangement of LEDs in the upper part, and (c) porcelain plaque placed in the lower part.

The device shown in Fig. 1 (a) has in its inner upper part, four ultrabright white LEDs (Bluex, 12 V, 1 W), which were used to control the light and an opening for the objective or lens from the digital camera or cell-phone camera, respectively, Fig. 1 (b). In the outer upper part, two variable resistors of 10 kΩ were used to supply a suitable electric current to the LEDs. An ON/OFF switch was used, as well as two connectors to the battery charger. The lower part contained the porcelain plaque (Fig. 1 (c)) and a rechargeable battery (Unipower, 12 V with 1.3 A h^{-1}) as power supply for the LEDs. The internal compartments of the system were painted matt black with a spray to eliminate reflection effects.

A Shimadzu spectrophotometer, model UV-vis 2550, with dual beam and quartz cuvette of 1.0 cm was used for ethanol spectrophotometric determination as the comparative method.

Chemicals and samples

The solutions were prepared with ultrapure water (resistivity > 18.0 MΩ cm) obtained from a Millipore Milli-Q system (USA), and all chemical reagents used were of analytical grade and without further purification. Ethanol of HPLC grade was purchased from Qhemis (Brazil). The ethanol stock solutions were prepared from the ethanol dilution in ultrapure water, with volumetric concentrations in the range 1.0% to 50.0% v/v (ethanol/water). The alcoholic drink samples were purchased in local supermarkets.

Digital image treatment

The captured images were analyzed using the freely available software ImageJ. In this software, a defined number of pixels from the digital image was selected (42 × 36), and these pixels were decomposed using the RGB approach, *i.e.*, values of mean and mode referent to the color channels red (R), green (G), and blue (B) partially absorbed by the solution and further reflected to the detector, and then imported to Excel® software.

According to the literature, several mathematical methods have been applied to use the RGB values acquired from the digital images.[19-35] However, an imprecision can be added in the method, if the blank value is not properly discounted. Because of this, a simple logarithmic equation similar to those employed in the calculation of transmittance in colorimetry has been reported.[28,31] As the R, G, or B values for the reaction (I) are lower than R, G, or B acquired from the blank (I_0), the –log (I/I_0) equation supplies the precise value ranged from 0 to 1 useful to construct the analytical curve.[28,31,36]

Optimization of operational parameters and calibration procedure

All operational parameters related to the image capture in the developed system (Fig. 1 (a)) as well as for the image treatment were systematically studied, including: the best *(i)* amount and *(ii)* position of the LEDs, *(iii)* LEDs intensity, *(iv)* use of flash from the devices, *(v)* solution volume in each vessel, *(vi)* amount of pixels correlated with the selected image area to RGB decomposition, and *(vii)* use of mean or mode values for the calculation of $-\log(I/I_0)$.

The device presented in Fig. 1 was calibrated using three dyes: brilliant blue, amaranth, and tartrazine, by observing the behavior for the R, G, and B channels, respectively, and to evaluate the homogeneity of lighting within the chamber. Analytical curves were obtained to determine the linear concentration range and analytical sensitivity for each dye and the respective channels.

Analytical procedure for ethanol determination

The colorimetric reaction used for the ethanol detection was based on the redox reaction of this compound with the

dichromate ion (Cr (VI)), generating acetic aldehyde and Cr (III) (green) or Cr (II) (blue), depending on the ethanol concentration, pH solution and the kinetic-reaction time. The reaction is presented in Eq. 1.

$$Cr_2O_7^{2-}{}_{(aq)} + 8H^+{}_{(aq)} + 3CH_3CH_2OH_{(l)} \rightarrow 2Cr^{3+}{}_{(aq)} + 3CH_3CHO_{(aq)} + 7H_2O_{(l)} \quad Eq.1$$

The reaction parameters were optimized. Thus, the type and concentration of the used acid, potassium dichromate concentration, reaction time, and volume of each reagent was evaluated. At this stage, the goal was to perform the reaction in the shortest possible time and with the highest sensitivity, as well as to produce a color scale that allowed a rapid screening analysis.

Under the optimum experimental conditions, the analytical curve for ethanol was obtained in triplicate from digital images captured for ethanol solutions with concentration in the range from 1.0% to 50.0% v/v. In contrast to the dyes where each R, G, and B channel has a maximum absorption, the images captured for ethanol solutions present a mixture of colors where any channel can be used, and so each channel (R, G, and B) was investigated.

Potential interferents in the ethanol colorimetric reaction were studied at a concentration ratio of ethanol to interferent of 1:1, 1:0.1, and 1:0.01. In addition, recovery tests were performed to verify the matrix effects.

Samples of beer, wine, vodka, and brandy ("cachaça") were analyzed using the proposed method and a spectrophotometric method. For the comparative method, the measurements were performed at λ_{max} of 350 nm that it was the wavelength of greater dichromate absorption. Thus, the method was employed to measure the fading color of dichromate solution, considering that the yellow color decreased with the ethanol concentration, and turned to green and blue colors proportionally to the increasing of the ethanol concentration.

Results and discussion

Optimization of operational parameters

Initially, the number of LEDs, as well as the disposition of these in the upper part of the device for the image capture, was evaluated. The best conformation of these components is shown in Fig. 1 (b), *i.e.,* four LEDs in the four corners of the top of the chamber. In this arrangement, a uniform illumination of the entire porcelain plaque was obtained. In addition, the LEDs intensity was studied using the variable resistors for each pair of LEDs. An intermediate condition for LED intensity was selected applying 6 V to each pair of LEDs, where the uniform illumination of the porcelain plaque was guaranteed. Thus, the negative effects were reduced, *i.e.,* the excess of bright and reflections from the LEDs; and the positive effects such as darkness or shadow due to poor or inefficient lighting. Next, the ideal total volume of the reaction vessels of the porcelain plaque was studied, with this volume adjusted to 835 µL. Using this selected volume, the problems relating to excessive brightness and reflections were minimized, and by using appropriate luminosity, the images showed a more homogeneous region, facilitating the selection of the area or number of pixels to be analyzed. Also, the use of flash for image capture was unnecessary, allowing the use of low-resolution digital cameras in which the flash is not present or has poor quality.

Regarding the DIB treatment step, the parameters optimized included the use of mean or mode values of each (R, G, and B) channel, and the size and position of the selected area to collect the R, G, and B values. When compared the methods of mean and mode, significant differences were not perceptible by analyzing of R, G, and B values. The number of the pixels selected was kept in function of the useful area that could be used, thus, a convenient value of 42 × 36 pixels was used for further experiments. Fig. S1 in Electronic Supplementary Information (ESI) is shown the selection of two different regions from a single image from a 1.0×10^{-4} mol L^{-1} amaranth solution, and in Table S1 the values of the mean and mode for the R, G, and B channels were showed. When the bright region was selected, not just the value of G, but also the R and B values increased, indicating less absorption of the three channels (R, G, and B). Thus, for further experiments, regions in the image that were without bright and shadow were selected.

Calibration of the system

For the calibration of the designed device, three dyes were used as standards: brilliant blue, amaranth, and tartrazine. Initially, exploratory analytical curves were constructed by evaluating the linear ranges for each dye and the variability among the R, G, and B channels. All channels responded to changing in the concentrations for all the dyes. However, after this study, we decided to monitor the channel in which the absorption maximum, *i.e.,* minimum reflectance, for each dye solution was verified: R channel for the brilliant blue, G channel for the amaranth, and B channel for the tartrazine. Fig. 2 presents the analytical curves obtained for the dyes using the cited channels using five different devices to capture the images. The analytical curves showed linear concentration range from 10 to 100 µmol L^{-1} with good correlation coefficients ($r \geq 0.99$).

Furthermore, from the analytical curves obtained using the different cameras with default configurations for each one, it was observed that it is possible to acquire good analytical performances using a digital camera with high resolution (and hence with high commercial value) or a simple camera from a cell phone to perform the image capture. However, it should be noted that the resolution parameter is not entirely negligible. In fact, when devices with a lower resolution are used, to obtain a good sensitivity and a precision close or equal to that achieved with a high-resolution device, a greater effective area of the photography of the sample should be selected to obtain a larger number of pixels needed for the image decomposition by the RGB system.

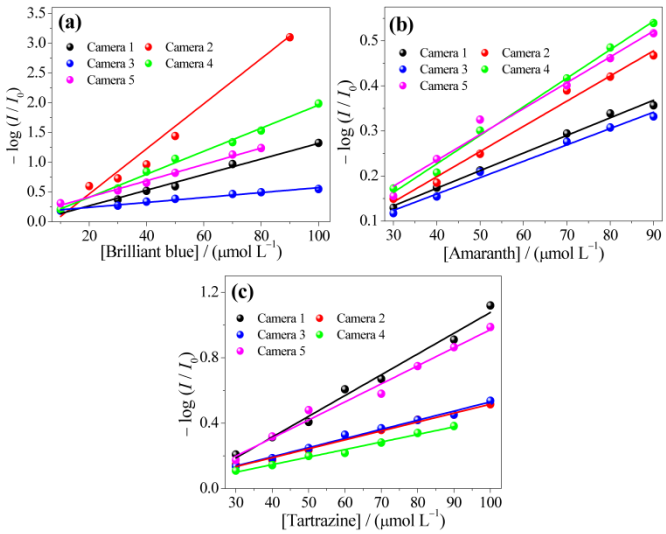

Fig. 2. Analytical curves obtained for the dyes (a) brilliant blue, (b) amaranth, and (c) tartrazine, using the five digital cameras. Sony 12.0 MP, model Cyber-shot (camera 1); Sony 6.0 MP, model DSC-W50 (camera 2); Fujifilm 5.1 MP, model FinePixA500S (camera 3); Samsung 2.0 MP, model GT-C6112 (camera 4, from a cell phone); and Aony 0.3 MP, model Q9 (camera 5, from a cell phone).

Optimization of reaction conditions

The influence of the type and concentration of the acid used in the colorimetric reaction was studied. Thus, sulfuric, nitric, and hydrochloric acids at concentrations of 18.0, 14.0, and 12.0 mol L^{-1}, respectively, were initially studied. Next, diluted solutions of sulfuric acid (1.8 and 3.5 mol L^{-1}), nitric acid (1.4 and 2.8 mol L^{-1}), and hydrochloric acid (1.2 and 2.4 mol L^{-1}) were investigated. Mixtures of concentrated hydrochloric and nitric acids 3:1 v/v, and concentrated sulfuric acid and hydrogen peroxide 3:1 v/v were also tested. In this study, analytical curves were obtained only when the concentrated acids, *i.e.*, sulfuric, nitric, or hydrochloric, were used. Sulfuric acid was selected because a lower reaction time was reached, and to obtain a wide scale of color. The concentrated sulfuric acid and hydrogen peroxide mixture 3:1 v/v rapidly reduced the Cr (VI) to Cr (II), generating an intense blue color in all reaction vessels of the porcelain plaque. On the other hand, when diluted acid solutions, or the concentrated hydrochloric and nitric acids mixture 3:1 v/v, were employed, the reaction was slower, and the color scale was not observed, with all vessels presented yellow shades, and a non-linear analytical curve was obtained.

In addition, the potassium dichromate concentration was evaluated. The following concentration values were investigated: 0.5, 0.1, 0.05, and 0.02 mol L^{-1}. The optimum potassium dichromate concentration was 0.05 mol L^{-1}. The use of high concentration values quickly provided intense colors, while the use of lower concentrations produced a discrete color scales, hindering an effective screening analysis.

Finally, the volume ratio between each reagent in the reaction vessels was optimized based on the optimum conditions that were previously obtained. Under the optimum experimental conditions, the following conditions were selected for obtaining the color scale: 640 µL of 0.05 mol L^{-1} potassium dichromate solution; 160 µL of standard or sample solution; and 35 µL of 18.0 mol L^{-1} sulfuric acid solution.

To evaluate the kinetics effect, the reaction time was varied in the range 0 to 30 min. Fig. 3 presents the captured images at different reaction times using a range of ethanol concentration from 1.0% to 50.0% v/v, thus making it possible to follow the reaction kinetics. The idea was to obtain a color scale according to the ethanol concentration (screening analysis).

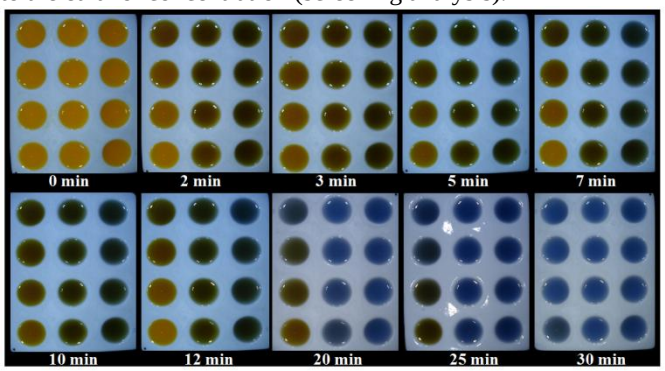

Fig. 3. Images of the porcelain plaque containing ethanol reactions with ethanol contents from 1.0% to 50.0% v/v at different reaction times.

As can be seen from Fig. 3, using shorter or longer reaction times, the method sensitivity reduced significantly. For shorter reaction times, the reactions in all reaction vessels showed yellow shades, and for longer reaction times the vessels showed blue shades. Therefore, a time of 12 min was selected for further studies, because in this condition, a good screening analysis could be performed as well as a quantitative determination of different ethanol concentrations by measurement of the variations in the R, G, and B channels.

Analytical features

As discussed, the resolution of the digital camera did not significantly influence the measurements. The analytical curve for ethanol was built using camera 2 (Sony 6.0 MP digital camera, model DSC-W50). Fig. 4 (a) shows an image of the porcelain plaque containing the colorimetric reactions for different ethanol contents, from 1.0% to 50.0% v/v. Fig. 4 (b) presents the analytical curve obtained from the treatment of the image shown in Fig. 4 (a) using the R channel. The G and B channels were also used in the image treatment of Fig. 4 (a), but linear regions were not identified (see Fig. S2 in the SI).

In Fig. 4 (b), two linear concentration ranges were obtained by monitoring the R channel. The first region ranged from 1.0% to 20.0% v/v and the second region from 25.0% to 50.0% v/v, following the linear regression equations:

First linear region: $-\log (I/I_0) = -0.016 + 0.029 \times$ [Ethanol] v/v, r = 0.999. Second linear region: $-\log (I/I_0) = 0.398 + 0.009 \times$ [Ethanol] v/v, r = 0.980.

Thus, the proposed method has a wide linear concentration range, thus is suitable for the determination of ethanol content in commercial alcoholic drinks. The limits of detection (LOD) and quantification (LOQ) were calculated using Eqs. 2 and 3:

$$LOD = 3\sigma_b/\beta \quad \text{Eq. 2}$$

$$LOQ = 10\sigma_b/\beta \quad \text{Eq. 3}$$

Where σ_b is the standard deviation of ten blank measurements and β is the slope of the analytical curve (sensitivity). The values determined were: LOD = 0.25% v/v and LOQ = 0.85% v/v. Moreover, as can be noted, a full calibration curve was obtained using only one digital image in a short time of 12 min.

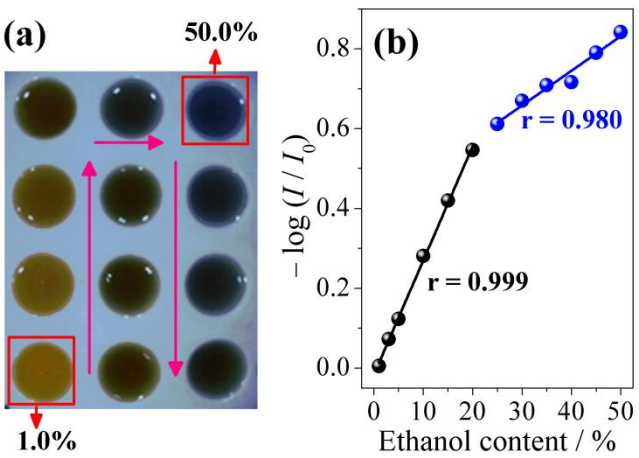

Fig. 4. (a) Image of the porcelain plaque containing ethanol reactions with ethanol contents from 1.0% to 50.0% v/v. The arrows indicate the direction of the ethanol content growth. (b) Analytical curves obtained for ethanol contents from 1.0% to 50.0% v/v and using the results from the R channel, including the two distinct linear regions.

Potential interferents such as: methanol, ethyl acetate and 2-butanone were evaluated for a 15% v/v ethanol solution at three different ratios ranged from 1:1, 1:0.1, to 1:0.01 (analyte/interferent). According to recovery tests, concentration ratio higher than 1:0.1 generated interference levels greater than 10%, only for methanol. Therefore, this concentration was considered the maximum tolerated for the proposed method. For ethyl acetate and 2-butanone the maximum tolerated ratio was 1:1. The methanol interference was expected because methanol have similar functional structures, and, therefore, similar reductive properties. However, this is not a problem, since the concentration of methanol in drinks and/or food is naturally negligible. Besides, this result is useful as indicative of adulteration or as parameter for quality control of alcoholic drinks, once the methanol should be present in low concentration.

Additionally, recovery studies were performed in order to evaluate possible sample matrix effects, Table 1. As can be seen, excellent recovery percentages were verified from 85.0% to 106%. Thus, the proposed method did not suffer significant matrix effects for ethanol determination.

Table 1. Ethanol recovery percentage for the commercial drink samples with $n = 4$.

Sample*	Added (% v/v)	Found (% v/v)	Recovery (%)
A	5.0	5.1 ± 0.7	102
	10.0	8.5 ± 0.5	85.0
B	5.0	5.1 ± 0.6	102
	10.0	9.2 ± 0.1	92.0
C	5.0	5.3 ± 0.3	106
	10.0	8.7 ± 0.5	87.0
D	5.0	4.7 ± 0.8	94.0
	10.0	9.1 ± 0.4	91.0
E	5.0	5.2 ± 0.5	104
	10.0	9.1 ± 0.5	91.0

*Beer, wine 1, wine 2, Vodka, Brandy (cachaça), respectively.

Applications

The developed method using a spot-test reaction associated with a digital image treatment was applied successfully for the ethanol determination in commercial alcoholic drink samples. Table 2 shows the results obtained for the sample analyses by the proposed and comparative methods. The developed method demonstrated to have a good accuracy and its effectiveness in the quantification of ethanol in commercial alcoholic drinks was confirmed. Moreover, the results obtained using the two methods were statistically compared using the paired t-test at a confidence level of 95%. The t_{exp} value (1.01) was smaller than the $t_{critical}$ value (2.57), and therefore, it can be concluded that there is no statistically significant difference between the results obtained using the two analytical methods.

Table 2. Results for the ethanol determination in commercial alcoholic drink samples by the DIB and comparative methods with $n = 6$.

Sample*	Spectrophotometric method (% v/v)	DIB method (% v/v)	Relative error (%)
A	6.63 ± 0.01	6.7 ± 0.4	+ 1.1
B	16.31 ± 0.07	17.7 ± 0.7	+ 8.5
C	22.07 ± 0.03	24.8 ± 0.8	+ 12.4
D	30.07 ± 0.08	26.3 ± 0.2	− 12.5
E	30.21 ± 0.05	28.2 ± 0.2	− 6.7

*Beer, wine 1, wine 2, Vodka, Brandy (cachaça), respectively.

Conclusions

A simple and low-cost procedure was proposed in this work for the quantification of ethanol in alcoholic drink samples, using a spot-test reaction and digital image treatment with an RGB approach. This work brings together the capabilities of the spot-test (quick response, low volume, and screening analysis) and digital images (portability, quantitative measures, low-cost instruments, and multivariate analysis, *i.e.*, three channels that can provide useful information).

The developed method was efficiently applied to the quantification of ethanol in commercial alcoholic drinks (beer, wine, vodka, and brandy "cachaça") samples. The proposed strategy can be employed for drink *in situ* analysis, *e.g.*, industry and smallholdings, due to the ease of handling and low-cost of the materials and portable instrumentation used. Additionally, a full calibration curve was obtained using only one digital image in a short time of 12 min, indicating the possibility of obtaining quick results of analysis with a low waste generation (835 µL/ spot-test). Thus, the DIB method is a useful tool regarding to environmental and social impacts, owing to its low waste generation and uses an easily available device with potential for *in situ* determination and/or quality control to alcoholic beverages products.

Acknowledgements

We gratefully acknowledge the Brazilian agencies FAPESP, CNPq and CAPES for financial support.

Notes and references

[a]Department of Chemistry, Federal University of São Carlos, Rod. Washington Luís km 235, P. O. Box 676 São Carlos-SP, Postal Code: 13560-970, Brazil. Email: vagnerlaqa@gmail.com. Phone: +55 11 30913781.

[b]Department of Physics, Chemistry and Mathematics, Federal University of São Carlos, Rod. João Leme dos Santos km 110, Sorocaba, CEP: 18052-780, SP, Brazil
[c]Institute of Exact Sciences and Technology, Federal University of Amazonas, Rua Nossa Senhora do Rosário 3863, Itacoatiara, CEP: 69103-128, AM, Brazil

Electronic Supplementary Information (ESI) available: See DOI: 10.1039/b000000x/

1. R. Singh, A. Shukla, S. Tiwari and M. Srivastava, *Renewable Sustainable Energy Rev.*, 2014, **32**, 713-728.
2. J. B. D. S. Ferreira-Filho and M. Horridge, *Land Use Policy*, 2014, **36**, 595-604.
3. C. Capello, U. Fischer and K. Hungerbuhler, *Green Chem.*, 2007, **9**, 927-934.
4. H. D. M. Avelar and P. J. S. Barbeira, *Fuel*, 2007, **86**, 299-302.
5. M. E. Charness, R. P. Simon and D. A. Greenberg, *N. Engl. J. Med.*, 1989, **321**, 442-454.
6. C. Guerri, *Alcohol: Clin. Exp. Res.*, 1998, **22**, 304-312.
7. S. V. Sumbhate, S. Nayak, D. Goupale, A. Tiwari and R. S. Jadon, *J. Anal. Tech.*, 2012, **1**, 1-6.
8. H. Nakamura, R. Tanaka, K. Suzuki, M. Yataka and Y. Mogi, *Food Chem.*, 2009, **117**, 509-513.
9. A. O. S. S. Rangel and I. V. Tóth, *Anal. Chim. Acta*, 2000, **416**, 205-210.
10. M.-L. Wang, Y.-M. Choong, N.-W. Su and M.-H. Lee, *J. Food Drug Anal.*, 2003, **11**, 133-140.
11. M. Gerogiannaki-Christopoulou, N. V. Kyriakidis and P. E. Athanasopoulos, *J. AOAC Int.*, 2003, **86**, 1232-1235.
12. AOAC, Alcohol in wines. By dichromate oxidation. 969. 12-1988.
13. P. Pinyou, N. Youngvises and J. Jakmunee, *Talanta*, 2011, **84**, 745-751.
14. P. J. Fletcher and J. F. Van Staden, *Anal. Chim. Acta*, 2003, **499**, 123-128.
15. T. F. M. Pais, S. S. M. P. Vidigal, I. V. Tóth and A. O. S. S. Rangel, *Food Control*, 2013, **30**, 616-620.
16. Ü. A. Kirgöz, D. Odaci, S. Timur, A. Merkoçi, S. Alegret, N. Beşün and A. Telefoncu, *Anal. Chim. Acta*, 2006, **570**, 165-169.
17. M. Hnaien, F. Lagarde and N. Jaffrezic-Renault, *Talanta*, 2010, **81**, 222-227.
18. G. Wen, Y. Zhang, S. Shuang, C. Dong and M. M. F. Choi, *Biosens. Bioelectron.*, 2007, **23,** 121-129.
19. L. Byrne, J. Barker, G. Pennarun-Thomas, D. Diamond and S. Edwards, *TrAC, Trends Anal. Chem.*, 2000, **19**, 517-522.
20. S. Paciornik, A. V. Yallouz, R. C. Campos and D. Gannerman, *J. Braz. Chem. Soc.*, 2006, **17**, 156-161.
21. Q. Li, Q. Xie, S. Yu and Q. Gao, *Food Hydrocolloids*, 2014, **35**, 392-402.
22. M. J. Deutsch, S. C. Schriever, A. A. Roscher and R. Ensenauer, *Anal. Biochem.*, 2014, **445**, 87-89.
23. S. Sumriddetchkajorn, K. Chaitavon and Y. Intaravanne, *Sens. Actuators, B*, 2013, **182**, 592-597.
24. I. A. Sima, D. Casoni and C. Sârbu, *Talanta*, 2013, **114**, 117-123.
25. A. D. P. M. da Silva, P. B. de Oliveira, T. B. Bandini, A. G. Barreto Junior, R. C. de Sena and J. F. C. da Silva, *Sens. Actuators, B*, 2013, **177**, 1071-1074.
26. A. W. Martinez, S. T. Phillips, E. Carrilho, S. W. Thomas, H. Sindi and G. M. Whitesides, *Anal. Chem.*, 2008, **80**, 3699-3707.
27. W. d. S. Lyra, L. F. da Almeida, F. A. S. Cunha, P. H. G. D. Diniz, V. L. Martins and M. C. U. de Araujo, *Anal. Methods*, 2014, **6**, 1044-1050.
28. S. K. Kohl, J. D. Landmark and D. F. Stickle, *J. Chem. Educ.*, 2006, **83**, 644.
29. K. L. Yam and S. E. Papadakis, *J. Food Eng.*, 2004, **61**, 137-142.
30. L. F. Oliveira, N. T. Canevari, M. B. B. Guerra, F. M. V. Pereira, C. E. G. R. Schaefer and E. R. Pereira-Filho, *Microchem. J.*, 2013, **109**, 165-169.
31. M. S. Gomes, L. C. Trevizan, J. A. Nóbrega and M. Y. Kamogawa, *Quim. Nova*, 2008, **31**, 1577-1581.
32. M. B. Lima, S. I. E. Andrade, I. S. Barreto, L. F. Almeida and M. C. U. de Araújo, *Microchem. J.*, 2013, **106**, 238-243.
33. W. d. S. Lyra, V. B. dos Santos, A. G. G. Dionízio, V. L. Martins, L. F. Almeida, E. d. N. Gaião, P. H. G. D. Diniz, E. C. Silva and M. C. U. de Araújo, *Talanta*, 2009, **77**, 1584-1589.
34. W. Wongwilai, S. Lapanantnoppakhun, S. Grudpan and K. Grudpan, *Talanta*, 2010, **81**, 1137-1141.
35. E. d. N. Gaiao, V. L. Martins, W. d. S. Lyra, L. F. d. Almeida, E. C. d. Silva and M. C. U. de Araújo, *Anal. Chim. Acta*, 2006, **570**, 283-290.
36. S. I. E. Andrade, M. B. Lima, I. S. Barreto, W. S. Lyra, L. F. Almeida, M. C. U. Araújo and E. C. Silva, *Microchem. J.*, 2013, **109**, 106-111.

